Expansion of research base/station in the Arctic

*Hiroyuki Enomoto[1]

1. National Institute of Polar Research

Arctic Challenge for Sustainability (ArCS) project coordinate the use of Arctic stations, research sites and facilities for ArCS colaborators and aloso Japanese researchers.
The sites are, IARC (International Arctic Research Center)/UAF and Poker Flat observation site in US, CHARS (Canadian High Arctic Research Station) and CEN (Centre for Northern Studies) in Canada, observation sites in Cape Baranocva and Spasskaya Pad in Russia, Ny-Alesund and UNIS (The University Centre in Svalbard) in Svalvard, Norway, EGRIP (East Greenland Ice Coring Project) site and GINR (Greenland Institute of Natural Resources) at Nuuk, Greenland.
These sites and facilities are available for research and training of young scientists.
The presentaion intoroduces the geographical distribution of pan-Arctic sites and their reseach targets, possible transfer to the social benefits, then discuss contribution to Japanese Arctic sciencific activities.

Keywords: Arctic, research sites, International scientific colaboration, international partnership

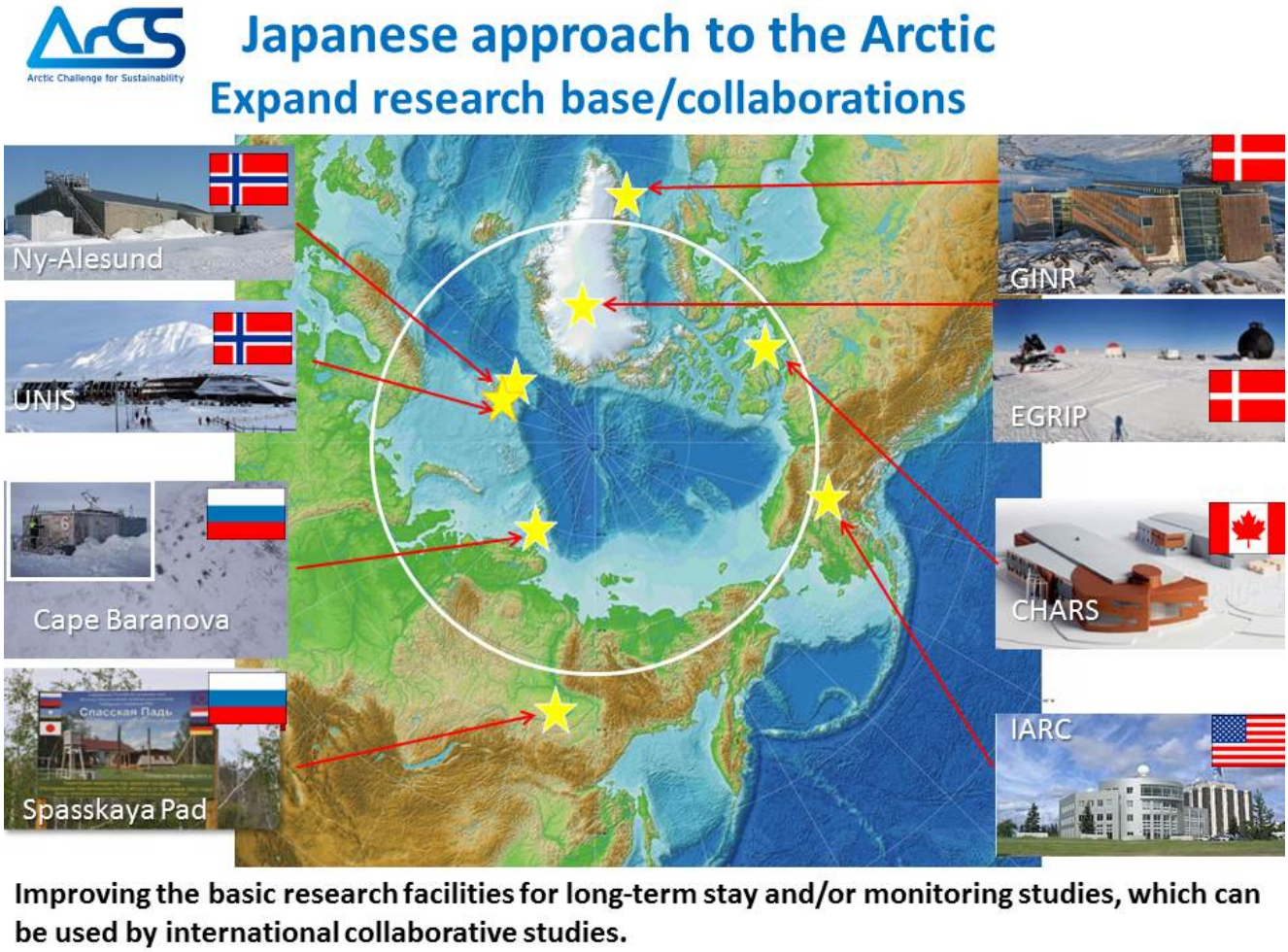

©2017. Japan Geoscience Union. All Right Reserved.

Water structures and circulation along with bio-geochemical processes in the Arctic Ocean suggested with nutrients and oxygen distributions

*Motoyoshi Ikeda[1,2], Shinichi Tanaka[3], Yutaka Watanabe[4]

1. Hokkaido University, 2. JAMSTEC, 3. Earthquake Research Institute, The University of Tokyo, 4. Graduate School of Earth Environmental Science, Hokkaido University

Climatological water mass structures were identified in the Arctic Ocean, using the geochemical dataset in the Hydrochemical Atlas of the Arctic Ocean (HAAC). In addition, a geochemically conserved parameter PO_4^* was considered under the following process: when the water column remineralization of organic matter occurs, the content of phosphate increases with decline of dissolved oxygen according to remineralization stoichiometry at the rate of $P:O_2 = 1: -175$ (Anderson and Sarmiento, 1994). The equation is formulated as
$PO_4^* = PO_4 + DO/175 - 1.95$ (μmol/L, Broecker, 1991)
Once the values of PO_4^* are very close to each other, there is high possibility that they have a common origin.
In the upper ocean above 500-m depth, as widely known from various datasets, the Pacific-origin Water (P-Water) is clearly indicated with higher silicate, higher phosphate and lower dissolved oxygen than the Atlantic-origin Water (A-Water). The boundary between the water masses is located along 135˚E-45˚W at the surface and rotates counter-clockwise with depth, confirming the anti-cyclonic circulation of P-Water in the surface layer (0 to 200-m depth), and the cyclonic circulation of A-Water in the subsurface layer (200 to 500-m depth), exchanging between the Arctic and the Atlantic oceans, caused by the water density contrast. Therefore, the HAAC dataset is reliable as a supplier of oceanographic information for a half century.
In the lower ocean below 1500-m depth with the basins separated by the Lomonosov Ridge, dissolved oxygen is lower in the Canadian Basin than the Eurasian Basin. The lower phosphate and higher dissolved oxygen are limited to the vicinity of the Barents Sea and the Fram Strait. Useful information was obtained from PO_4^* (Table below): i.e., the lower-ocean water is maintained by a descending flow along the Siberian continental slope coming from the Atlantic through the Barents Sea, in addition to penetration of the Nordic Seas Deep Water flowing from the Greenland Sea. The former component circulates cyclonically to the Canadian Basin, as shown with PO_4^* =0.65~0.67, along with the high core of PO_4^* =0.86 at 2000m-depth in the southern Canada Basin under the influence of the shelf water. The latter component with PO_4^* =0.72 spreads along the sea floor (3500-m depth) from the Atlantic side to the Pacific side.
The lower-ocean water mass gradually receives nutrients from sinking organic matters, and provides the intermediate-layer water between the upper and the lower oceans. The intermediate water is mostly occupied with A-Water and entrains water from the subsurface portion also, returning toward the Atlantic.
Anderson and Sarmiento, 1994: *Global Biogeochemical Cycles*, **8**, 65-80.
Broecker, 1991: *Oceanography*, **4**, 79-89.
Table: The values of PO_4 and DO taken from the horizontal maps with rounding at 2%. The unit is μmol/L. The values are confirmed with the vertical profiles.

Keywords: Arctic Ocean, geochemical tracer, remineralization, ocean circulation

©2017. Japan Geoscience Union. All Right Reserved.

Location	PO_4	DO	PO_4*
Northern boundary of Barents Sea (200m & 500m)	0.85	310	0.67
Canadian Basin excluding high PO_4 area (2000m) & all (2500m)	1.00	280	0.65
Canada Basin in high PO_4 area (2000m)	1.15	290	0.86
Eurasian Basin (2000m & 2500m)	0.95	300	0.72
Greenland Sea Fram Strait (500m)	0.70	340	0.69
Greenland Sea Fram Strait (2000m)	0.70	310	0.52

©2017. Japan Geoscience Union. All Right Reserved.

Nutrient Dynamics Affecting Phytoplankton Distributions in the Pacific Arctic Region

*Shigeto Nishino[1], Takashi Kikuchi[1], Michiyo Yamamoto-kawai[2], Yusuke Kawaguchi[1], Toru Hirawake[3], Motoyo Itoh[1], Amane Fujiwara[1], Michio Aoyama[4,1]

1. JAMSTEC Japan Agency for Marine-Earth Science and Technology, 2. Tokyo University of Marine Science and Technology, 3. Hokkaido University, 4. Fukushima University

The Chukchi Sea and Canada Basin are areas in the Pacific Arctic characterized by northward advection and spreading of Pacific-origin water that transports nutrients into the Arctic Ocean, and thus plays an important role in phytoplankton distributions. In this study, we examined ship-based and mooring data to understand nutrient dynamics and its influence on phytoplankton distributions. In the southern Chukchi Sea, our data suggest that, in contrast to spring blooms that are caused by a nutrient supply with the advection of Pacific-origin water, autumn blooms there are maintained by regenerated nutrients from the bottom of the shallow sea where particulate organic matters are largely accumulated in autumn. On the other hand, large-scale ocean circulation controls nutrient distributions in the Canada Basin where sea ice reduction in recent years has changed the ocean circulation and thus impacts on the nutrient and phytoplankton dynamics. We found that oceanographic and biological responses to the sea ice loss are quite different between the Alaskan and Siberian sides of the region. On the Alaskan side, eddies also play an important role in the nutrient and phytoplankton distributions. However, on the Siberian side, data are still lacking and various biogeochemical processes should be clarified in future studies.

Keywords: Arctic Ocean, Sea ice reduction, Ocean circulation, Eddy, Nutrients, Phytoplankton

©2017. Japan Geoscience Union. All Right Reserved.

Species invasion and diversity in benthic macrofaunal communities in the Pacific Arctic

*Hisatomo Waga[1], Toru Hirawake[2], Jacqueline M Grebmeier[3]

1. Graduate School of Fisheries Sciences, Hokkaido University, 2. Faculty of Fisheries Sciences, Hokkaido University, 3. Chesapeake Biological Laboratory, University of Maryland Center for Environmental Science

There is growing evidence of increased Pacific water transport into the Arctic that is influenced by variations in atmospheric forcing. One of the empirical and theoretical predictions for a future Arctic impacted by increased Pacific water transport is that new taxa will expand or invade the Arctic ecosystem. However, well-documented examples are still scarce due to the limited number of time-series measurements in the Arctic, particularly for benthic organisms. Although benthic organisms are normally stationary and less mobile than fishes, seabirds and mammals, it seems relevant that benthic organisms with pelagic life stages will be less limited in their expansion abilities. In this study, the relationship between the number of benthic macrofaunal taxa and atmospheric forcing was investigated in the Pacific Arctic. Average taxon number of benthic macrofauna for 2010–2012 has increased significantly compared to 2000–2006 on the continental shelf area from south of St. Lawrence Island in the northern Bering Sea to just north of St. Lawrence Island in the Chirikov Basin, likely caused by the difference in magnitude and location of the Aleutian Low. By comparison, the biomass-based Shannon-Weaver diversity index did not reflect the changes in taxon number of benthic macrofauna. These results indicate increased invasion of new taxa into the region for 2010–2012 compared to 2000–2006, but the biomass of new taxa is negligible when compared with the total benthic macrofaunal biomass. Our findings demonstrated indications of ongoing changes that could continually be facilitated by climate change to future Arctic marine ecosystems in the Pacific Arctic region.

Keywords: Arctic, Benthic community, Pacific water transport

©2017. Japan Geoscience Union. All Right Reserved.

Evaluation of riverine heat inflow in the Arctic Ocean modeling

*Eiji Watanabe[1], Hotaek Park[1], Tatsuo Suzuki[1], Dai Yamazaki[1]

1. Japan Agency for Marine-Earth Science and Technology: JAMSTEC

River water is known as important sources of freshwater and nutrients in the Arctic Ocean. Its spatial distribution has been widely visualized using observed chemical properties and numerical tracer experiments. However, continuous monitoring of the volume flux is limited only at major river stations. A substantial amount of uncertainties still remains particularly on ungauged rivers. We compared a couple of river water discharge datasets in the Arctic Ocean modeling. The Arctic Ocean Model Intercomparison Project (AOMIP) traditionally adopted monthly climatology of 13 major rivers, which was based on the R-ArcticNET data archive. The ungauged inflow was added under simple assumption. A daily discharge dataset covering most Arctic sea coasts and multiple decades was recently developed by combining land runoff of the Japanese 55-year reanalysis for driving ocean and sea ice models (JRA55-do) and drainage of the Catchment-based macro-scale floodplain scheme (CaMa-Flood). Another daily discharge dataset was provided using the coupled hydrological and biogeochemical model (CHANGE) and the Total Runoff Integrating Pathways scheme version 2 (TRIP2). An originality of the third dataset is explicit calculation of river ice and snow loading so that the gridded data of river water temperature are also available.
In this study, to evaluate an impact of riverine heat inflow on sea ice in the Arctic Ocean, decadal experiments for 1979–2013 were performed using the Center for Climate System Research Ocean Component model version 4.9 (COCO4.9) in the pan-Arctic regional framework. The horizontal grid size was set to approximately 25 km, and atmospheric forcing components were constructed from the National Centers for Environmental Prediction–Climate Forecast System Reanalysis (NCEP–CFSR). First, the riverine volume inflow was given by three datasets, respectively, so that the sensitivity of sea ice and hydrography was checked. The model results in these cases showed similar interannual variability of sea ice thickness and sea surface salinity in each sub-domain (e.g., Kara and Beaufort seas). We then incorporated the river water temperature into the model experiment. The annual mean sea ice thickness in this case produced negative anomaly over the Siberian shelves and in the southern Canada Basin. The seasonal transitions in sea ice concentration and sea surface temperature indicated that riverine heat inflow into the Arctic Ocean accelerated summer sea ice opening and sea surface warming in the vicinity of major river mouths.

Keywords: Arctic Ocean model, land–ocean interaction, river water temperature, sea ice melting

©2017. Japan Geoscience Union. All Right Reserved.

Variability of sea-ice thickness in the northeastern coastal Chukchi Sea revealed by a moored ice-profiling sonar

*Yasushi Fukamachi[1], Daisuke Simizu[2], Kay I. Ohshima[1], Hajo Eicken[3], Andrew R. Mahoney[3], Katsushi Iwamoto[4], Erika Moriya[5], Sohey Nihashi[6]

1. Hokkaido University, 2. National Institute of Polar Research, 3. University of Alaska Fairbanks, 4. City of Mombetsu, 5. Hydro Systems Development, Inc., 6. National Institute of Technology, Tomakomai College

Using a moored ice-profiling sonar, time-series ice-draft data were obtained in a coastal region of the northeastern Chukchi Sea during 2009-10 for the first time. Time-series data show seasonal growth of sea-ice draft, which is occasionally interrupted by the appearances of coastal polynya and upwelled Atlantic Water.The sea-ice draft distribution indicates the abundance of thicker ice comparable or less than in the adjacent Beaufort Sea.The rapid increase of thicker ice from December to January corresponded to the minimal offshore drift in January and the resulting rapid decrease of level-ice fraction indicating dynamical thickening processes.The mean draft and its converted thickness are 1.27 and 1.54 m, respectively. Heat losses are calculated with ice-thickness data averaged over various time scales corresponding to various spatial scales. Comparing to the estimate with ice-thickness data every second, these estimates are roughly two thirds and a half for the cases with spatial averaging over ~20 and 100 km, respectively.The heat-loss estimate based on thin-ice data derived from the AMSR-E corresponds well with the estimate based on the 1-second observed ice-thickness data, indicating the validity of a thin-ice thickness algorithm and the resulting heat-loss estimate based on the AMSR-E data.

Keywords: sea-ice thickness, Chukchi Sea, ice-profiling sonar

©2017. Japan Geoscience Union. All Right Reserved.

Can the anticyclonic eddy trap and amplify near-inertial waves in the Arctic Ocean?

*Eun Yae Son[1], Yusuke Kawaguchi[2], Jae-Hun Park[1], Ho Kyung Ha[1]

1. Inha University, 2. JAMSTEC

The hydrographic data obtained by the Ice-Tethered Profiler with Velocity (ITP-V) were utilized to reveal the eddy-internal wave interaction in the Canada Basin, Arctic. The ITP-V is an autonomous drifting instrument that collects profiles of hydrographic data and velocity concurrently in depths of 10-250 m at 3-hr interval. The observation using the ITP-V, installed on the multi-year sea ice, was operated for 9 months from August 2014. We focus on a specific event in mid-October, when a near-surface anticyclonic eddy was observed in depths of 50-100 m. The anticyclonic eddy showed vertically stretched isopycnals with anomalously warm water in its core. It is noted that the near-inertial internal waves were trapped and amplified near the bottom of the eddy, where the horizontal and vertical wave lengths were approximately 10 km and 60 m, respectively. The parameterized turbulent diffusivity (Gregg, 1989) reached up to 10^{-5} m^2/s near the bottom of the eddy while the background diffusivity was around 10^{-7} m^2/s. Our results demonstrate that near-inertial waves can be trapped and amplified within the anticyclonic eddy in the Arctic and can enhance the ocean mixing like mid latitudes.

Keywords: Near-inertial internal waves, anticyclonic eddy, fine-scale parameterization, Canada Basin

©2017. Japan Geoscience Union. All Right Reserved.

Interannual salinity variations in the northwestern Bering Sea associated with the Bering Strait throughflow

*Yoshimi Kawai[1], Satoshi Osafune[1], Shuhei Masuda[1], Yoshiki Komuro[2]

1. Research and Development Center for Global Change, Japan Agency for Marine-Earth Science and Technology, 2. Institute of Arctic Climate and Environment Research, Japan Agency for Marine-Earth Science and Technology

The relationship between the Bering Strait throughflow (BTF) and sea surface salinity (SSS) in the Bering Sea was investigated mainly using an atmosphere-ocean-ice coupled model, MIROC4h, which includes an eddy-permitting ocean model. The MIROC4h simulated well the seasonal cycle of BTF transport, although it overestimated the transport compared with mooring-based estimates. The interannual variations of SSS in the Bering Sea were correlated with those of BTF transport: SSS in the northwestern Bering Sea was high when BTF transport was large. And there was seasonality in the relationship between SSS and BTF. The SSS anomaly associated with the BTF anomaly became evident from winter to spring, and SSS lagged behind the BTF by a few months. Similar relationship between the BTF and SSS can be seen in an observation dataset and two kinds of ocean data assimilation product, although there were some differences from the MIROC4h in the spatial distribution and the timing of large *r*. Sea surface temperature (SST) also became higher with the larger BTF transport in the cold season, however, the surface density were affected by the SSS anomalies more than the SST ones. BTF transport was strongly correlated with SSH in the eastern Bering Sea, the southwestern Chukchi Sea (CS), and the East Siberian Sea (ESS); there was no time lag between the BTF and SSH. The low SSH along the Siberian coast was uncorrelated with the high SSH in the Bering Sea. The Arctic SSH affected BTF transport and the SSS in the northwestern Bering Sea independently of the SSH in the Bering Sea. The *r* between the SSH and zonal wind stress suggested that shelf waves might be excited by zonal wind anomalies in the Laptev Sea or north of the New Siberian Islands to propagate to the Bering Strait. The low SSH along the Siberian coast associated with high SSS in the northwestern Bering Sea, however, was not confirmed in 10 years of satellite-derived SSH data. The relationship between the Arctic SSH and SSS in the Bering Sea still needs to be further investigated.

We evaluated the salt budget in the northwestern Bering Sea using the MIROC4h data. When the BTF transport in October–March was large, the horizontal salt advection increased and meltwater decreased; both changes contributed to the mixed-layer salinization, but the horizontal advection term dominated north of 62.5˚N, and the sea-ice melting term did south of 62.5˚N. The residual term, which mainly represented eddy diffusion, had a role to suppress the magnitude of the salinity tendency. The same features can be seen when the SSH in the southwestern CS and the ESS was low in the cold season. In these cases, the near-surface current anomalies across the contours of salinity were reinforced, and the horizontal salt convergence occurred in the northwestern part of the Bering Sea. Furthermore, the anomalous southerlies and currents contributed to the sea-ice retreat. The SSH anomalies in the Arctic Ocean affected the currents in Bering Strait and the northwestern Bering Sea, perhaps through the propagation of shelf waves, to lead to the salinization. The current anomalies in the northwestern part associated with the BTF or SSH anomalies became weaker in the warm season, which produced the seasonality of the correlation.

Keywords: Bering Strait throughflow, sea surface salinity, sea surface height, MIROC4h

©2017. Japan Geoscience Union. All Right Reserved.

Subglacial meltwater discharge and its impact on water properties in Bowdoin Fjord, northwestern Greenland

*Yoshihiko Ohashi[1,2], Shigeru Aoki[2], Yoshimasa Matsumura[2], Shin Sugiyama[2,3], Naoya Kanna[3], Daiki Sakakibara[3], Yasushi Fukamachi[2,3]

1. Graduate School of Environmental Science, Hokkaido University, 2. Institute of Low Temperature Science, Hokkaido University, 3. Arctic Research Center, Hokkaido University

Meltwater runoff from the Greenland ice sheet to the ocean has increased in recent years. Thus, it is important to assess the impact of meltwater runoff on the oceanic structure. In marine-terminating glaciers, subglacial meltwater discharge occurs at the grounding line depth and forms an upwelling plume. To understand the impact of subglacial meltwater discharge on water properties, we carried out CTD observations in Bowdoin Fjord, northwestern Greenland in the summers of 2014 and 2016. A numerical experiment of subglacial meltwater plume was also performed with a non-hydrostatic ocean model to examine the effects of freshwater flux changes.
In ocean observations of 2014 and 2016, a significantly high turbidity layer (> 5 FTU) was observed at the subsurface of 20–40 m depth, which was caused by subglacial meltwater plume. Moreover, the level of turbidity and potential temperature showed interannual variations: turbidity was higher and temperature was lower near the surface (5–15 m depth) in 2016, whereas turbidity was lower and temperature was higher at the layer below (50–100 m depth). The observed structure suggests that a larger discharge of turbid subglacial meltwater in 2016, with a larger buoyant force, mixed with the fjord water at the grounding line depth and extended at the relatively shallower depths. The situation is consistent with the fact that the sum of positive degree days at Qaanaaq Airport, a proxy for meltwater runoff in this region, was approximately 20% greater in 2016 than in 2014. In the numerical experiment with 20% greater amount of freshwater flux, concentration of a meltwater tracer near the surface increased by roughly 20% from that of the control case, whereas the tracer concentration decreased at the layer below. The difference in the vertical distribution of tracer concentration with and without increasing the freshwater flux was consistent with that of turbidity in the two years. These results indicate that the change in amount of subglacial meltwater runoff affects the behavior of turbid subglacial meltwater plume and material transport, which might further impact on biogeochemical cycles.

Keywords: Glacier-ocean interaction, Subglacial meltwater plume, Water properties, Fjord, Greenland

©2017. Japan Geoscience Union. All Right Reserved.

Characterizing landscape-scale distribution of sparse larch forest and surrounding wetland in Taiga-Tundra boundary ecosystem, Northeastern Siberia

*Tomoki Morozumi[1], Atsuko Sugimoto[2,1], Ryo Shingubara[1], Shinya Takano[1], Ruslan Shakhmatov[1], Rong Fan[1], Shunsuke Tei[2], Hideki Kobayashi[3], Rikie Suzuki[3], Trofim C Maximov[4,5]

1. Graduate School of Environmental Science, Hokkaido University, 2. Arctic Research Center, Hokkaido University, 3. Department of environmental geochemical cycle research, JAMSTEC, 4. Institute for Biological Problems of Cryolithozone SB RAS, 5. BEST center, North Eastern Federal University

Vegetation cover is essential information for upscaling GHG emission in local to regional scale. Taiga-Tundra boundary ecosystem consists of sparse Larch forest and polygonal wetland in eastern Siberia, and it is no easy task to know the structure of heterogeneous landscape. Field observation and high resolution satellite image provide information for vegetation cover on a microtopographic level, while coarser resolution image contains mixed pixels. To evaluate fraction of small vegetation patch, subpixel classification has been applied at coarser resolution satellite image. In this study ALOS AVNIR2 (JAXA) reflectance image (70 x 70 km) was classified into landscape unit and then subpixel vegetation cover was obtained by linear spectral unmixing (LSU) method based on vegetation endmember of field reflectance and tree distribution survey in Indigirka lowland eastern Siberia (70°N, 148°E) in July summer. Result was validated by higher resolution vegetation map that was derived from WorldView-2 (Digital Globe) for 10 x 10 km.

AVNIR2 image was classified into 15 landscape units by ISODATA unsupervised classification. Each landscape unit in 10m resolution AVNIR2 image contained usually 2 to 4 dominated vegetation classes in 2-0.5 resolution WorldView-2 vegetation map. For example, a landscape unit near tributary consisted of Sedge, Shrub and smaller fraction such as Tree and Salix endmembers. After endmember collection, subpixel vegetation cover was estimated for 70 x 70km scale, and it revealed landscape-scale distribution and zonation of vegetation cover in Taiga-Tundra boundary. Prior to this study, we have investigated CH4 emission and biomass production of willow bush for 10 x 10km local scale in this observation area. This subpixel vegetation data will allow us to upscale these parameters on biogeochemical cycles for larger spatial scale.

Keywords: vegetation, landscape, subpixel classification

©2017. Japan Geoscience Union. All Right Reserved.

Highly Dynamic Methane Emission from the West Siberian Boreal Floodplains

Irina Terentieva, Alexander Sabrekov[1,2], Ali Ebrahimi[3], Mikhail Glagolev[1,2,4,5], *Shamil S Maksyutov[6]

1. Tomsk State University, 36 Lenina Street, Tomsk 643050, Russia, 2. Institute of Forest Science, Russian Academy of Sciences, 21 Sovetskaya st., Uspenskoe, Moscow region 143030, Russia, 3. Department of Environmental Systems Science, ETH Zurich, 8092 Zurich, Switzerland, 4. Yugra State University, 16 Chekhova st., Khanty-Mansyisk 628012, Russia, 5. Moscow State University, 1 Leninskie gory, Moscow 119992, Russia, 6. National Institute for Environmental Studies, 16-2 Onogawa, Tsukuba, Ibaraki, 305-8506, Japan

Methane production from riparian wetlands may cause significant CH4 emissions to the atmosphere. However, seasonal floodplains of many high-latitude rivers are still not represented in studies on methane emissions. A major river in West Siberia is Ob River; it is one of the longest rivers in the world. Despite its potential importance, field observations of the CH4 fluxes in that domain were mainly focused on peatlands and lakes. The present study is a first attempt to estimate variability of methane fluxes from West Siberian boreal floodplains. Results of the study can be used for further data upscaling, especially in combination with floodplain area data.

Methane emission measurements were made by static chamber method during 2015-16 summer periods. Test sites were located at the Ob River floodplain near Khanty-Mansiysk city, Russia, as well as within smaller floodplains in taiga zone.

Flux medians varied in two orders of magnitude from zero to 17.5 mgC/m^2/h. Aiming at further upscaling, we managed such heterogeneity by classifying studied environments with following criteria: i) floodplain width (small or large), ii) microrelief (elevated or depressed), iii) inundation during the measurements («wet» or «dry»). Within this framework, several classes were found to be similar in CH_4 emission rates: i) «wet» and «dry» depressions of large floodplains had highest fluxes of 4.21 mgC/m^2/h with interquartile range (IQR) of 5.17 mgC/m^2/h, ii) «wet» elevations within large floodplains and all small «wet» floodplains had lower flux median of 1.47 mgC/m^2/h with IQR of 2.99 mgC/m^2/h, iii) «dry» elevations within large floodplains and all small «dry» floodplains had the lowest median of 0.07 mgC/m^2/h with IQR of 0.26 mgC/m^2/h.

This observations highlight high variability of emission, which is most evident in depressions within large floodplains, where a few rare but large emission events can contribute significantly to the total emission rates. It was also found that there were only slight difference between emissions from «wet» and «dry» depressions. It can be related to the presence of constant overwetting due to close position of underground waters or water accumulation after precipitation periods.

Besides the common variability of methane fluxes, we also observed «hot moments» of methane emission. In particular, time-series measurements at Ob floodplain revealed sudden peak in emissions just after the main water subsiding (comparing to the fluxes during the flooding period). Results also indicated gradual decreasing of emissions and its dispersion from 5.89 mgC/m^2/h to 3.51 mgC/m^2/h during two weeks of soil drying. We hypothesize that gas bubbles were initially accumulated in soil during the inundated period when the gas diffusion rate was limited and hydrostatic pressure was high. Such accumulation was confirmed by dissolved CH4 concentration measurements in sediments revealing 10 times higher CH4 concentration in comparison with the water column. We suggested that further methane release could be triggered by abrupt hydrostatic pressure decrease induced by water drawdown. Since the threshold concentration of dissolved methane correlates with the water column depth, water level drop might lead to gas generation from the solution and the enlargement of the volume of the gas phase with further

©2017. Japan Geoscience Union. All Right Reserved.

ebullition.
As the next step, we need systematic measurements of methane fluxes and their combining with floodplain mapping for further data upscaling.

Keywords: welands, methane, greenhouse gasses, arctic, Siberia

©2017. Japan Geoscience Union. All Right Reserved.

Assessing and projecting greenhouse gas release from dynamic permafrost degradation

*Kazuyuki Saito[1], Hiroshi Ohno[2], Tokuta Yokohata[3], Go Iwahana[4], Hirokazu Machiya[1]

1. Japan Agency for Marine-Earth Science and Technology, 2. Kitami Institute of Technology, 3. National Institute for Environemtal Studies, 4. University of Alaska Fairbanks

Permafrost is a large reservoir of frozen soil organic carbon (SOC; about half of all the terrestrial storage). Therefore, its degradation (i.e., thawing) under global warming may lead to a substantial amount of additional greenhouse gas (GHG) release. However, understanding of the processes, geographical distribution of such hazards, and implementation of the relevant processes in the advanced climate models are insufficient yet so that variations in permafrost remains one of the large source of uncertainty in climatic and biogeochemical assessment and projections. Thermokarst, induced by melting of ground ice in ice-rich permafrost, leads to dynamic surface subsidence up to 60 m, which further affects local and regional societies and eco-systems in the Arctic. It can also accelerate a large-scale warming process through a positive feedback between released GHGs (especially methane), atmospheric warming and permafrost degradation. This three-year research project (2-1605, Environment Research and Technology Development Fund of the Ministry of the Environment, Japan) aims to assess and project the impacts of GHG release through dynamic permafrost degradation through in-situ and remote (e.g., satellite and airborn) observations, lab analysis of sampled ice and soil cores, and numerical modeling, by demonstrating the vulnerability distribution and relative impacts between large-scale degradation and such dynamic degradation. Our preliminary laboratory analysis of ice and soil cores sampled in 2016 at the Alaskan and Siberian sites largely underlain by ice-rich permafrost, shows that, although gas volumes trapped in unit mass are more or less homogenous among sites both for ice and soil cores, large variations are found in the methane concentration in the trapped gases, ranging from a few ppm (similar to that of the atmosphere) to hundreds of thousands ppm We will also present our numerical approach to evaluate relative impacts of GHGs released through dynamic permafrost degradations, by implementing conceptual modeling to assess and project distribution and affected amount of ground ice and SOC.

Keywords: Ice-rich permafrost degradation, Methane, climate change, tipping point

©2017. Japan Geoscience Union. All Right Reserved.

Assessing and projecting greenhouse gas release from dynamic permafrost degradation 【ERTDF 2-1605 FY2016-18】

環境省

Model improvement, Projections

・Quantification of potential methane release
・Refined future climate projections
etc.

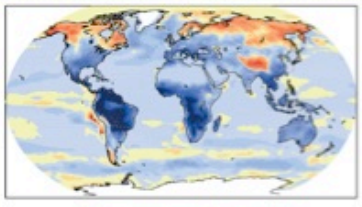

Previous studies
Incremental and kinetic degradation
→Need to incorporate local but dynamic degradation

Sub theme 3 :
Projecting future gas release by integrated land surface model with explicit permafrost dynamics (NIES)

Understanding of vulnerability (remote-sensing, numerical modeling)

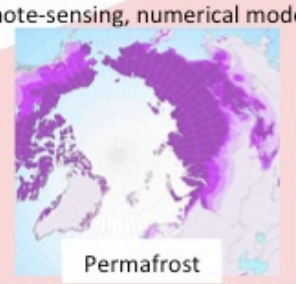

Ice-rich permafrost

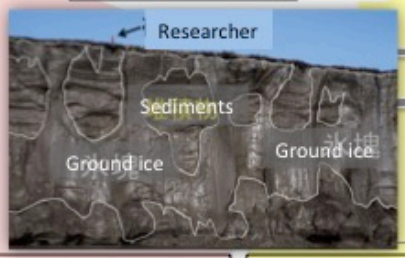

Sampling and lab-analyses of methane in ice cores

Sub theme 1 :
Assessing dynamic permafrost degradation mechanism and vulnerability (JAMSTEC)

Sub theme 2 :
Quantifying organic carbon content (GHG) in large permafrost ice and sediments (Kitami Inst. of Technology)

©2017. Japan Geoscience Union. All Right Reserved.

Impact of Arctic sea ice decline on recently observed climate change: a coordinated multi-model study

*Noel S Keenlyside[1,2,3], Fumiaki Ogawa[1,3], HoNam Hoffman Cheung[1,3], Yongqi Gao[2,3,1], Torben Koenigk[4], Vladimir Semenov[5], Lingling Suo[2,3], Shuting Yang[6], Tao Wang[7], Martin Peter King[8,3], Guillaume Gastineau[9], Sergey Gulev[10]

1. Geophysical Institute, University of Bergen , 2. Nansen Environmental and Remote Sensing Center, 3. Bjerknes Cente for Climate Research, 4. Swedish Meteorological and Hydrological Institute, Sweden, 5. Helmholtz centre for ocean research Kiel GEOMAR, Germany, 6. Danish Meteorological Institute, Denmark, 7. Insititute of Atmospheric Physics, China, 8. Uni-Research Climate, Norway, 9. Sorbonne universities, France, 10. Shirshov Institute of Oceanology, Russia

To what extent the recent sea-ice decline influenced Northern Hemisphere climate trends remains an open question. To address this we perform two atmospheric general circulation model experiments: In both experiments observed daily sea ice cover variations are prescribed for the period 1982 to present, while for SST, one experiment uses observed daily variations and the other the observed climatology. The experiment is performed by six different state-of-the-art AGCMs. Our results show that the observed wintertime temperature trend near the surface is poorly reproduced. The impact of SIC variation seems to be confined near the surface, while SST variation seems a key for temperature trend above. This suggests a necessity to consider the atmospheric poleward energy transport associated with SST variation to understand the observed arctic amplification. The simulations fail to reproduce the observed changes in the Siberian High and Eurasian wintertime cooling. Northern hemisphere surface and zonal mean tropospheric temperature trends are better reproduced in boreal autumn, but the impact of sea ice decline remains limited to the lower troposphere. Other aspects of SIC/SST impact on the observed circulation change such as NAO shall also be discussed.

Keywords: Sea ice decline, Climate Change, Sea ice impact

©2017. Japan Geoscience Union. All Right Reserved.

Evaluation of Atmospheric Response to Arctic Sea Ice Anomalies

*Masato Mori[1]

1. Research Center for Advanced Science and Technology, the University of Tokyo

During the last decade, severe winters occurred frequently in mid-latitude Eurasia, despite increasing global- and annual-mean surface air temperature. Statistical analyses of observational data have suggested that some part of these cold winters were forced by Arctic sea-ice decline. However, numerical modelling studies have shown different conclusion depending on the used model and experimental settings, and whether or not the cause is due to sea ice reduction is controversial. Therefore, it is important to clarify the cause of the diversity of simulation results, especially the extent to which sea ice anomaly controls the atmospheric circulation.
In this research, we successfully detected the signature of Eurasian cold winters excited by sea-ice decline in the Barents-Kara Sea, by generating a four kind of long-term historical and large-member ensemble simulation based on atmospheric general circulation model (AGCM). The sea ice reduction tends to increase occurrence frequency of cold winter over the central Eurasia, but its effect may have been underestimated in the AGCM. We conclude that this is one of the big reasons that conclusion change depending on model experiments.

Keywords: sea ice, the Arctic, cold winter

©2017. Japan Geoscience Union. All Right Reserved.

Baroclinic Wave Response to the Arctic Amplification of Global Warming

*Hiroshi Tanaka[1], Makoto Sakurai[2]

1. Center for Computational Sciences, University of Tsukuba, 2. School of Life and Environmental Science, University of Tsukuba

The Arctic warms twice faster than the global average of the warming trends. This response to the global warming is called Arctic Amplification (AA). Pronounced AA occurs in fall to winter seasons due to the ice-albedo feedback, cloud feedback, and the enhanced meridional heat and moisture transports. The meridional transports are accompanied by baroclinic waves in mid-latitudes, and the transports are expected to decrease by the AA owing to the reduced baroclinicity. The purpose of this study is to investigate the changing baroclinic instability in response to the AA by means of the theoretical linear stability analysis. According to the result of the analysis, the growth rate of the baroclinic waves decreases by the AA. The structure of baroclinic waves changes so as to reduce the eddy momentum transport to the polar jet in high latitudes. It is found that a positive feedback exists between the weaker polar jet and reduced eddy momentum transport to the jet in association with the AA.

Keywords: Arctic amplification, Baroclinic instability waves, Linear stability analysis, Baroclinic eddies, Eddy momentum transport

©2017. Japan Geoscience Union. All Right Reserved.

Interannual variation of snow grain size on Greenland ice sheet retrieved from MODIS data –difference between Terra, Aqua and their composite –

*Teruo Aoki[1,2], Rigen Shimada[3], Tomonori Tanikawa[2], Masashi Niwano[2], Hiroshi Ishimoto[2], Masahiro Hori[3], Knut Stamnes[4], Wei Li[4], Nan Chen[4]

1. The Graduate School of Natural Science and Technology, Okayama University, 2. Meteorological Research Institute, Japan Meteoological Agency, 3. Earth Observation Research Center, Japan Aerospace Exploration Agency, 4. Department of Physics and Engineering Physics, Steven Institute of Technology

Surface albedo in accumulation area of Greenland ice (GrIS) sheet mainly controlled by variation of snow grain size because snow impurity concentration is low. Recent warming in the Arctic could accelerate snow metamorphism and thus bring snow grain growth. Possible cause of recent darkening in accumulation area of GrIS is snow grain growth, which has a positive feedback to the further warming in the Arctic. Satellite remote sensing is an efficient tool for monitoring of snow parameters. However, long-term variation of satellite sensor sensitivity may affect the retrieval result of grain size as well. MODIS onboard Terra and Aqua is one of the most suitable satellite sensors to retrieve snow grain size, but it is reported that the sensor degradation of Terra/MODIS is more significant than Aqua/MODIS (Polashenski et al., 2015). Hence, it could affect the long-term variation of snow grain size retrieved. Recently, sensor sensitivity-corrected data set of Terra and Aqua/MODIS (C6) were released (Lyapustin et al., 2014). Using these data, we retrieved surface snow grain size (Rs1) on GrIS from Terra and Aqua independently, with the algorithm based on a look-up table (LUT) method (Stamnes et al., 2007) at the wavelength of 1.24 μm. The LUT for bidirectional reflectance distribution function was calculated with a radiative transfer model for the atmosphere-snow system (Aoki et al., 2000) using a snow shape model employing Voronoi columns and aggregates (Ishimoto et al., 2012).

To analyze long-term variation of Rs1, monthly mean for all snow-covered area in GrIS was calculated from monthly mean image of Rs1, which is calculated from the daily images of Rs1 on GrIS. Comparing monthly mean Rs1 between Terra and Aqua, the monthly mean values of Rs1 derived from Terra were slightly smaller than those from Aqua. The differences are almost less than 10%. Since the year of launch differs between Terra and Aqua, we compared the interannual trend of Rs1 during the same period from 2003 to 2016 for Terra and Aqua. Both interannual trends from April to September agree well each other. Then, we calculated composite Rs1 from Terra and Aqua, by which we investigated variation of Rs1 for 2000-2016. The result shows that interannual trend of Rs1 is the largest (+32 μm/decade) in July and small positive in April, May, June and August, and negative in September. However, this situation changes for plateau area higher than 3 km, for which the largest interannual trend of Rs1 is relatively small (+14 μm/decade) in July and furthermore small positive in April, May, June and August, and small negative in September. These results means the snow surface grain size on GrIS has an increasing tend except for September during 2000-2016 and thus contributes to albedo reduction.

References

Aoki et al., 2000: *J. Geophys. Res.*, **105**, 10219-10236, doi:10.1029/1999JD901122.
Ishimoto et al., 2012: J. Quant. Spectrosc. Radiat. Transfer, 113, 632-643, doi:10.1016/j.jqsrt.2012.01.017.
Lyapustin et al., 2014, Atmos. Meas. Tech., 7, 4353–4365, doi:10.5194/amt-7-4353-2014.

©2017. Japan Geoscience Union. All Right Reserved.

Polashenski et al., 2015, *Geophys. Res. Lett.*, **42**, doi:10.1002/2015GL065912.
Stamnes et al., 2007, *Remote Sens. Environ.,* **111**, 258-273, doi:10.1016/j.rse.2007.03.023.

Keywords: snow grain size, albedo, Greenland ice sheet, satellite remote sensing, MODIS

©2017. Japan Geoscience Union. All Right Reserved.

Variations in Sr and Nd isotopic ratios of mineral particles in cryoconite in western Greenland

*Naoko Nagatsuka[1], Nozomu Takeuchi[2], Jun Uetake[1], Rigen Shimada[3], Yukihiko Onuma[4], Sota Tanaka[2], Takanori Nakano[5]

1. National Institute of Polar Research, 2. Chiba University, 3. JAXA, 4. University of Tokyo, 5. Waseda Univesity

Recently, the area of dark-colored ice has expanded and reduced surface albedo on the Greenland Ice Sheet. One of the possible causes of dark ice expansion is an increase in cryoconite, which is a dark colored surface dust consisting of mineral particles and organic matters. In order to better understand the source and transportation process of minerals on the dark-colored ice, we analyzed the Sr and Nd isotopic ratios of minerals in cryoconite, which were collected from glaciers in northwest and southwest Greenland.
The mineral components of the cryoconite showed variable Sr and Nd isotopic ratios, which corresponded to those of the englacial dust and moraine on and around the glaciers but were significantly different from those of the distant deserts that have been considered to be primary sources of mineral dust on the Greenland Ice Sheet. This suggests that the minerals within the cryoconites were mainly derived from local sediments, rather than from distant areas. The Sr ratios in the northwestern region were significantly higher than those in the southwestern region. This is probably due to geological differences in the source areas, such as the surrounding glaciers in each region.
The isotopic ratios further varied spatially within a glacier (Qaanaaq and Kangerlussuaq areas), indicating that the minerals on the glaciers were derived not from a single source but from multiple sources, such as englacial dust and wind-blown minerals from the moraine surrounding the glaciers.

Keywords: Greenland, Darkening of glaciers , Sr and Nd isotopic ratios, Mineral source

©2017. Japan Geoscience Union. All Right Reserved.

Meltwater floods at Qaanaaq ice cap in northwestern Greenland investigated by using a surface mass balance model

*Daiki Sakakibara[1,2], Masashi Niwano[3], Shin Sugiyama[2]

1. Arctic Research Center, Hokkaido University, 2. Institute of Low Temperature Science, Hokkaido University, 3. Physical Meteorology Research Department, Meteorological Research Institute

Melt increase in the Greenland ice sheet and peripheral ice caps give impact on coastal environment, but only a few studies have focused on its influence on the human activity in Greenland. Qaanaaq, a village in northwestern Greenland populated by 500 people, has been a base for field campaigns conducted by the GRENE and ArCS projects. On 21 July 2015 and 3 August 2016, streams flooded in the village, which resulted in destruction of a road between the village and Qaanaaq Airport. These floods were caused by increased runoff from Qaanaaq ice cap located several kilometers from the village. Similar floods were recorded in the past, but the one in 2016 caused unusually serious damage. Possibly, these floods are the results of recently changing climatic conditions in the Arctic region.
In this study, we investigated the floods in 2015 and 2016 by using a surface mass balance model NHM-SMAP (*Niwano et al.*, 2012, 2014). Model output at 5 km mesh grid points was downscaled to a 300 m grid, using the method proposed by *Noël et al.* (2016). This method considers the dependence of snow and ice melt rate on elevation. Digital elevation model and ice mask provided by Byrd Polar and Climate Research Center were used for this procedure (*Howat et al.*, 2014). We compared downscaled surface mass balance with the observational data acquired in 2012–2016. Then we estimated the amount of runoff from Qaanaaq ice cap.
Runoff from Qaanaaq ice cap was significantly larger than usual on 21 July 2015 and 2 August 2016, the day and the previous day of the flood in 2015 and 2016, respectively. The runoff computed for 21 July was the second greatest in 2015. Daily mean air temperature observed at Qaanaaq airport showed the highest in the year during the period from 21 to 23 July. In the upper part of the ice cap, the largest amount of melting in the year was calculated on the day of the flood. No significantly large melting was computed after the flood in 2015. Runoff on 2 August was the third largest in 2016, which corresponds to the largest amount of daily rainfall. From these results, rapid melting and strong rainfall were suggested as the causes of the floods in 2015 and 2016, respectively. This study showed that the floods occurred in the end of melt season.

References

Howat, I. M., A. Negrete, and B. E. Smith (2014), The Greenland Ice Mapping Project (GIMP) land classification and surface elevation data sets, *Cryosphere*, **8**, 1509–1518.
Niwano, M., T. Aoki, K. Kuchiki, M. Hosaka, and Y. Kodama (2012), Snow Metamorphism and Albedo Process (SMAP) model for climate studies: Model validation using meteorological and snow impurity data measured at Sapporo, Japan, *J. Geophys. Res.*, **117**, F03008.
Niwano, M., T. Aoki, K. Kuchiki, M. Hosaka, Y. Kodama, S. Yamaguchi, H. Motoyoshi, and Y. Iwata (2014), Evaluation of updated physical snowpack model SMAP, *Bull. Glaciol. Res.*, **32**, 65-78.
Noël, B., W. J. van de Berg, E. van Meijgaard, P. Kuipers Munneke, R. S. W. van de Wal, and M. R. van den Broeke (2015), Evaluation of the updated regional climate model RACMO2.3: Summer snowfall impact on the Greenland Ice Sheet, *Cryosphere*, **9**(5), 1831–1844.

Keywords: Greenland, Glacier, Surface mass balance model, Flood

©2017. Japan Geoscience Union. All Right Reserved.

©2017. Japan Geoscience Union. All Right Reserved.